Ethylcellulose Based Nanosponges as Drug Carriers for Febuxostat

Omnya M. Amin[*], Amal A. Ammar, Shereen A. Eladawy

Department of Pharmaceutics and Industrial Pharmacy, Faculty of Pharmacy, Al Azhar University, Girls Branch, Cairo, Egypt

www.ijppr.humanjournals.com

Keywords: Emulsion solvent diffusion method, Febuxostat, Gout, Nanosponge, Sustained release

ABSTRACT

Purpose: Febuxostat, a xanthine oxidoreductase inhibitor, is a drug of choice for gout. It is available as an immediate-release formulation in the market. The objective of the present study was to produce a sustained release of Febuxostat nanosponge. **Methods:** Nanosponges containing Ethyl cellulose as a polymer were prepared successfully using Polyvinyl alcohol as surfactant by Emulsion Solvent Diffusion Method. The effects of different ratios of polymer and surfactant on production yield, entrapment efficiency, particle size and *in vitro* release were studied. Nanosponge formulations that released (≥30 %) at 1st hour followed by controlling the release (≥75%) at six hours were further evaluated via SEM, Zeta-potentials, DSC and FTIR techniques. **Results:** SEM illustrates a porous and sponge-like structure. DSC and FTIR studies confirmed the formation of nanosponge and encapsulation of Febuxostat within it. The Zeta-potentials were high (-21.5 mV). The particle sizes were between 21.31 and 162.2 nm. The *in vitro* release study showed a sustained release pattern. **Conclusions:** Sustained release nanosponge formulations of Febuxostat have successfully been prepared.

INTRODUCTION

Febuxostat is a non-purine selective inhibitor of xanthine oxidase, the enzyme which oxidizes both hypoxanthine and xanthine to uric acid, excess of which is responsible for the gout disease. Although, the oral route for Febuxostat is extensively accepted but it is coupled with contraindicative manifestations such as less oral bioavailability because of its short biological half-life with significant fluctuations in plasma concentrations as it belongs to low solubility class (class II) of the Biopharmaceutical Classification System (BCS) and therefore require higher and frequent dosing which results in increased frequency of adverse effects [1]. To counter these problems, different types of sustained release dosage forms have been proposed and developed. Various sustained-release mechanisms such as diffusion, dissolution, osmotic pressure, pH and ion exchange resin-drug complexes can be employed to modulate the release of drug from the dosage form. However, these systems are associated with several limitations, e.g. stability issues, toxicity due to dose dumping, gastric irritation, instability at acidic pH, high cost and less dose adjustment [2]. To overcome these problems, the focus has been drawn towards nanotechnological approaches, where the release of the drug can be controlled in a more precise manner. It has brought about the development of new techniques in drug formulations one of which is the nanosponge (NS). NS is one of the colloidal carriers (nano-sized) that have been currently suggested for the effective delivery of the drug. It is a novel approach that offers controlled drug delivery to the active site which contributes towards reduced side effects, increased stability, targeted delivery, taste masking and ease of formulation [3]. Nanosponges are a three-dimensional network-like structure. The polymer is combined with crosslinkers acting as small hooks to join various parts of the polymer chains together. The overall effect is the formation of spherical microscopic particles comprising countless interconnecting cavities having the ability to encapsulate a wide range of drug substances [4]. The porous nature of the outer surface of the sponge offers control on the release of drug from the dosage form. Drug candidates having certain characteristics e.g. molecular weight between 100-400, solubility less than 10 mg/mL and melting point less than 250 °C are considered ideal for such type of preparations [5]. This work focused on the encapsulation of Febuxostat in nanosponges as a new formulation using Ethylcellulose, Polyvinyl alcohol as a surfactant for sustaining the release of the drug.

Citation: Omnya M. Amin et al. Ijppr.Human, 2019; Vol. 16 (4): 309-322.

310

MATERIALS AND METHODS

Febuxostat (FEB) powder was kindly provided by HIKMA Pharm Company, Cairo (Egypt). Dichloromethane (DCM) and Polyvinyl alcohol (PVA) was purchased from Pharma Middle East Company, German. Ethyl alcohol was supplied from El-GOMHOURIA Company, Cairo (Egypt). Ethylcellulose (EC) was kindly provided by EPICO pharm Company, Cairo (Egypt). All other reagents and chemicals used were of analytical grade. Double distilled water was used throughout the studies.

SYNTHESIS OF FEBUXOSTAT NANOSPONGE SYSTEM

In this method, two phases of organic and aqueous (Ethylcellulose and Polyvinyl alcohol) are used for preparing twelve formulae. The dispersed phase having FEB (40 mg) which was dissolved in DCM (10 ml) and EC in different proportions (1:2, 1:4, 1:6 and 1:8 FEB: EC) which were dissolved in 15 ml DCM. The aqueous continuous phase containing PVA in different concentrations (0.2, 0.4 and 0.6 %) to which the dispersed phase was slowly added. Then, the mixture is stirred properly at 1800 rpm for 2 hours. The required NS were collected by the process of filtration and kept for drying in the oven at 40 ºC for 24 hours. NS which are dried were stored in desiccators to ensure the removal of residual solvents.

EVALUATION OF THE PREPARED FEBUXOSTAT NANOSPONGES

Determination of Percentage Production Yield of Nanosponges:

The percentage production yield of the prepared NS was determined by calculating accurately the initial weight of the raw materials and the last weight of the NS obtained after drying [6].

$$\text{Production Yield (\%)} = \left(\frac{\text{Practical mass of Nanosponge}}{\text{Theoretical mass}}\right) \times 100$$

Determination of Percentage Entrapment Efficiency:

The drug content in the prepared FEB-NS was determined using a UV spectrophotometer. A weighed amount of the prepared FEB-NS was dissolved in 10 ml Ethanol and centrifuged (Superspin, USA) at 10,000 rpm for half an hour, then the supernatant was withdrawn in 100 ml volumetric flask and was completed to 100 ml with phosphate buffer (pH 6.8). The solution was subsequently diluted by taking 3 ml of it in 50 ml volumetric flask and complete to 50 ml with phosphate buffer (pH 6.8), then spectrophotometric absorbance was measured

Citation: Omnya M. Amin et al. Ijppr.Human, 2019; Vol. 16 (4): 309-322.

311

at 315 nm. The drug content was calculated from the calibration curve and expressed as percent entrapment efficiency [7].

$$\text{Entrapment Efficiency (\%)} = \left(\frac{\text{Actual drug content}}{\text{Theoretical drug content}}\right) \times 100$$

Particle Size Determination:

Zeta sizer (DTS Ver. 4.10, Malvern Instruments, UK) was used to determine the average particle size of the NS. The sample of dispersion was diluted 1:9 v/v with deionized water. The mean hydrodynamic diameter of the particles was calculated using the cumulated analysis after averaging the three measurements.

In Vitro **Dissolution Study and Kinetic Modelling of Drug Release:**

The *in vitro* drug dissolution was carried out using the USP Dissolution Apparatus II. An accurately weighed amount of each NS formulae equivalent to 40 mg of FEB was placed in 900 ml of dissolution medium (phosphate buffer, pH 6.8) at 37 °C ± 0.5 °C with a rotation speed of 75 rpm. Aliquots, each of (5 ml) of the sample were withdrawn from the dissolution medium at time intervals of 1, 2, 3, 4, 5, 6, 7, 8 and 24 hours by using a pipette. The same volume of phosphate buffer (pH 6.8) was used to replace the samples withdrawn to maintain the sink condition. The samples were suitably filtered, diluted and assayed spectrophotometrically at 315 nm. From this, the mean cumulative % of drug released was calculated from the previously constructed standard calibration curve and plotted against the function of time to study the pattern of drug release. Each test was performed in triplicate (*n* = 3) [8]. The release kinetics of FEB from different NS formulae was evaluated by employing the Korsmeyer Peppa's equation. Kinetic studies were performed by adjusting the release profiles to Higuchi, First, and Zero order equations. The kinetic parameters and correlation coefficient were calculated for the *in vitro* dissolution of all formulae [9].

Zeta Potential Determination:

The zeta potential of the selected NS was determined by Laser Doppler Anemometry using a Malvern Zeta sizer (Malvern Instrument, UK) also called Doppler Electrophoretic Light Scatter Analyzer using specific electrode containing cuvettes at concentrations of 20 mg/ml.

Citation: Omnya M. Amin et al. Ijppr.Human, 2019; Vol. 16 (4): 309-322.

312

Surface Morphological Study:

The surface morphology of the selected NS was determined using an analytical scanning electron microscope (JSM-6360A, JEOL, Tokyo, Japan). The samples were lightly sprinkled on a double adhesive tape stuck to an aluminum stub. The stubs were then coated with platinum to a thickness of about 10 A° under an argon atmosphere using a gold sputter module in a high-vacuum evaporator. The stub containing the coated samples was placed in the scanning electron microscope chamber [10].

Fourier Transform Infrared Spectroscopy (FTIR):

Fourier transform infrared spectrometer (Perkin-Elmer, FTS-1710, Beaconsfield, (UK)) was used. In this study, the potassium bromide disc method was employed. Pure FEB, physical mixture of FEB and EC (PM) and the selected NS formula were studied in the region of 4,000 cm^{-1} –400 cm^{-1} to confirm the formation of NS and encapsulation of FEB. The provided samples were then compressed into a transparent disc under high pressure using the special disc. The disc was placed in the IR spectrometer using a sample holder and the spectrum was recorded [10].

Differential Scanning Calorimetry (DSC):

The thermal characteristics of Pure FEB, physical mixture of FEB and EC (PM) and the selected NS formula were determined by Differential scanning calorimetry (Shimadzu, model DSC-50, (Japan)). Samples were weighed and placed in a sealed aluminum pan. An empty aluminum pan was used as a reference. The purity determination was performed using a heating rate of 5 °C/min. in the temperature range from 30-300 °C in a nitrogen atmosphere with a flow rate of 30 ml/min. The data were calculated in three replicates by Shimadzu TASYS software. DSC was preliminary calibrated with a standard of indium [10].

RESULTS

Determination of Percentage Production Yield of Nanosponges:

The percentage practical yield value of NSs was ranged from 44.44±1.43 % to 70.87±1.34% as shown in Table 1. It was found that the percentage of practical yield was increased with an increase in EC and PVA concentration.

Citation: Omnya M. Amin et al. Ijppr.Human, 2019; Vol. 16 (4): 309-322.

313

Determination of Percentage Entrapment Efficiency:

The percentage entrapment efficiency of NS was ranged from 73.41±3.21 % to 94.53±3.28 % as shown in Table 1. It was observed that the percentage of entrapment efficiency was increased with an increase in EC concentration and decrease PVA concentration.

Particle Size Determination:

The mean particle size of NS was ranged from 21.31±5.65 to 162.2±10.76 nm as shown in Table 1. All the nanosponge formulations showed particle sizes in the nano range (< 1 μm).

Table No. 1: Percent production yield, Percent entrapment efficiency and Particle sizes of the Febuxostat loaded nanosponges

Formulae	Percent production yield Mean ± SD	Percent entrapment efficiency Mean ± SD	particle size (nm) Mean ± SD
EC_1	44.44 ± 1.43	78.71 ± 2.11	21.31±5.65
EC_2	51.83 ± 4.51	81.93 ± 5.21	49.37±11.85
EC_3	57.89 ± 4.89	88.76 ± 3.78	95.33±8.52
EC_4	53.93 ± 6.32	94.53 ± 3.28	112±9.13
EC_5	46.21 ± 1.54	74.98 ± 3.56	55.42±7.48
EC_6	53.76 ± 4.21	80.03 ± 2.54	79.56±5.67
EC_7	64.43 ± 3.21	86.16 ± 1.76	122±3.78
EC_8	62.71 ± 5.11	93.22 ± 3.65	159.2±14.76
EC_9	48.8 ± 2.54	73.41 ± 3.21	68.43±18.12
EC_{10}	55.61 ± 2.77	78.90 ± 6.32	89.56±7.69
EC_{11}	70.87 ± 1.34	81.82 ± 6.55	120.51±17.89
EC_{12}	65.77 ± 1.89	91.63 ± 6.72	162.2±10.76

In Vitro **Dissolution Study and Kinetic Modelling of Drug Release:**

A biphasic release pattern of FEB was observed in Figures 1,2 & 3. The observed initial burst release was ranged (from 16±3.44 % to 30.41±2.03 %) followed by sustained release of the drug for 24 hours. The plain Febuxostat was dissolved within 3 hours. The mean values of correlation coefficients (r) were higher according to the Higuchi-Diffusion order. The release exponent values of all the formulations obtained were from 0.209 to 0.483 as shown in Table 2.
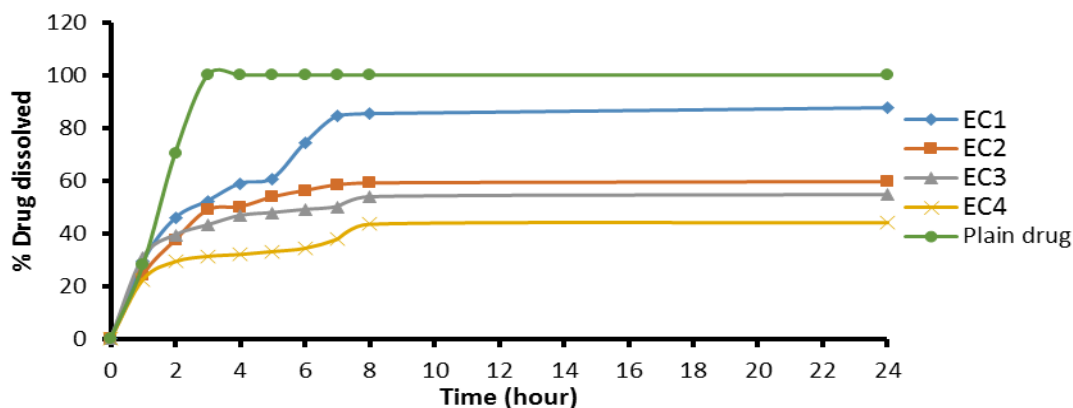
Citation: Omnya M. Amin et al. Ijppr.Human, 2019; Vol. 16 (4): 309-322.

314

Figure No. 1: *In vitro* dissolution of Febuxostat loaded nanosponges EC_1, EC_2, EC_3 and EC_4 and plain drug in phosphate buffer (pH 6.8)
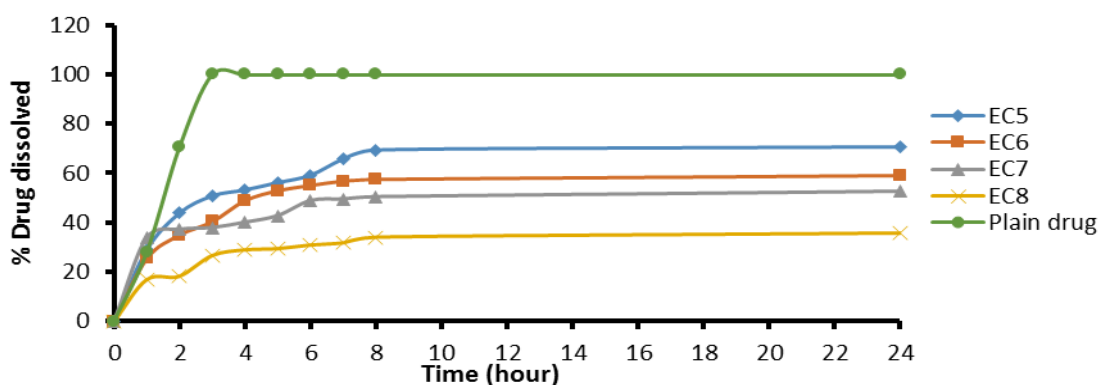

Figure No. 2: *In vitro* dissolution of Febuxostat loaded nanosponges EC_5, EC_6, EC_7 and EC_8 and plain drug in phosphate buffer (pH 6.8)
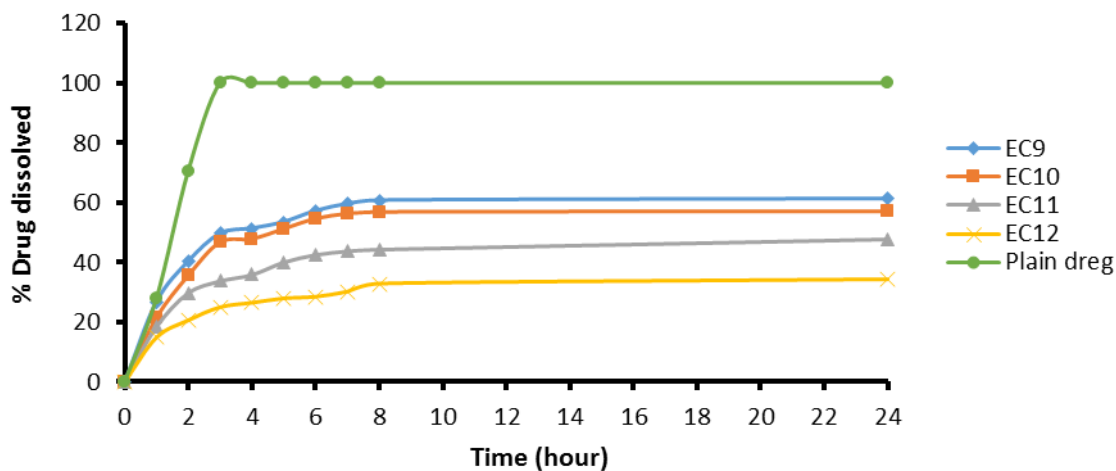

Figure No. 3: *In vitro* dissolution of Febuxostat loaded nanosponges EC_9, EC_{10}, EC_{11} and EC_{12} and plain drug in phosphate buffer (pH 6.8)

Citation: Omnya M. Amin et al. Ijppr.Human, 2019; Vol. 16 (4): 309-322.

315

Table No. 2: The calculated correlation coefficient (r) and (n) value for the Febuxostat loaded nanosponges based on *In vitro* dissolution study

Formula	Correlation coefficient (r)				(n) value
	Zero-order	First-order	Higuchi-diffusion model	Korsmeyer peppa's model	
Plain drug	0.905655	-0.741659	0.972617	0.842498217	0.495718
EC$_1$	0.968307	0.670137	0.998153	0.98985828	0.482867
EC$_2$	0.933139	0.781870	0.990695	0.959783808	0.398414
EC$_3$	0.91239	0.796588	0.982957	0.98737611	0.242363
EC$_4$	0.931183	0.802624	0.98793	0.962309444	0.275943
EC$_5$	0.943584	0.754553	0.9947518	0.985576417	0.382913
EC$_6$	0.941454	0.773942	0.99430	0.989602175	0.398915
EC$_7$	0.911433	0.791917	0.9808578	0.954307349	0.209496
EC$_8$	0.938030	0.7996354	0.992387	0.965954992	0.359005
EC$_9$	0.928411	0.7739135	0.989890	0.967813622	0.36036
EC$_{10}$	0.934186	0.7767593	0.990827	0.954902906	0.424955
EC$_{11}$	0.941536	0.7895806	0.994259	0.978259619	0.397584
EC$_{12}$	0.935565	-0.974533	0.987594	0.991468643	0.33021

Zeta Potential Determination:

Zeta potential of the selected EC$_1$ was –21.5 mV as shown in Figure 4.
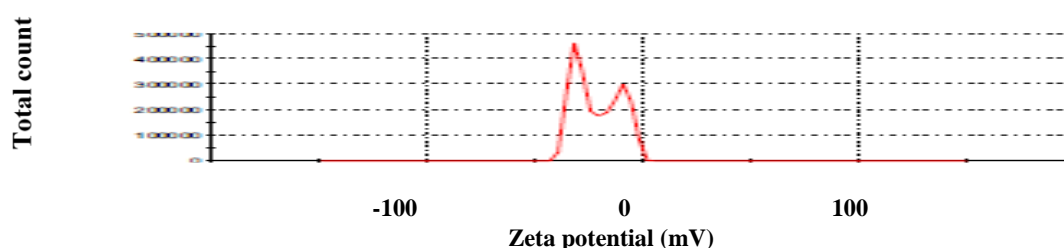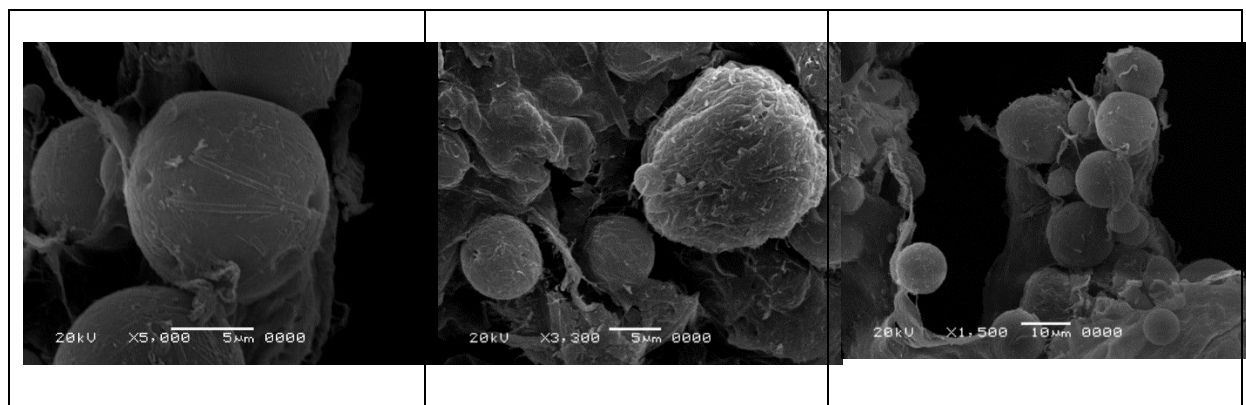

Figure No. 4: The zeta potential of the selected formula of Febuxostat loaded nanosponges (EC$_1$)

Surface Morphological Study:

Scanning Electron Microscopy of the selected EC$_1$ illustrated spherical uniform shape with a spongy structure as shown in Figure 5.

Citation: Omnya M. Amin et al. Ijppr.Human, 2019; Vol. 16 (4): 309-322.

316

Figure No. 5: Scanning electron microscopy photographs of the selected formula of Febuxostat loaded nanosponge (EC$_1$)

Fourier Transform Infrared Spectroscopy (FTIR):

Figure 6 shows an IR spectrum of FEB alone (a) which was characterized by absorption bands at high frequency at 2958.80 cm^{-1} and 2873.94, most probably attributed to the C-H stretching band of alkanes group, and at 2646.34 cm^{-1} and 2546.04 cm^{-1} were due to carboxylic acid O-H stretch. The peak observed at 2231.57 cm^{-1} was due to nitrile C≡N stretch. Peaks at 1678.07 cm^{-1}, 1604.77 cm^{-1}, 1508.33 cm^{-1}, and 1280.73 cm^{-1} were due to aryl carboxylic acid C=O stretching, C=N stretching of thiazole ring, C=C stretching of the ring and C-O-C stretching of ether group, respectively. Aromatic bending was observed from 763.81 cm^{-1}. Figure 6 (b) shows the FTIR spectrum of a physical mixture of FEB and EC (PM). All characteristic peaks of FEB were experiential in the IR spectra of the physical mixture. Figure 6 (c) shows the FTIR spectrum of the selected NS formula (EC$_1$) which is characterized by the disappearance of the absorption bands at high frequency at 2958.80 cm^{-1} most probably attributed to the C-H stretching band of alkanes group and at 2646.34 cm^{-1} were due to carboxylic acid O-H stretch. Also, there was shifting and broadening of peaks at 1678.07 cm^{-1} to 1689.64 cm^{-1} were due to aryl carboxylic acid C=O stretching and at 1280.73 cm^{-1} to 1288.45 cm^{-1} were due to C-O-C stretching of ether group.

Citation: Omnya M. Amin et al. Ijppr.Human, 2019; Vol. 16 (4): 309-322.

317

a
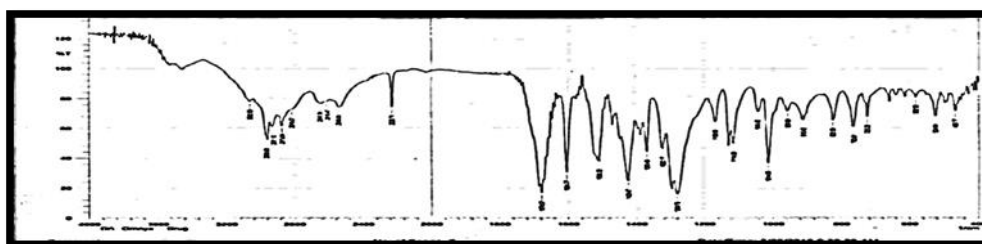
b
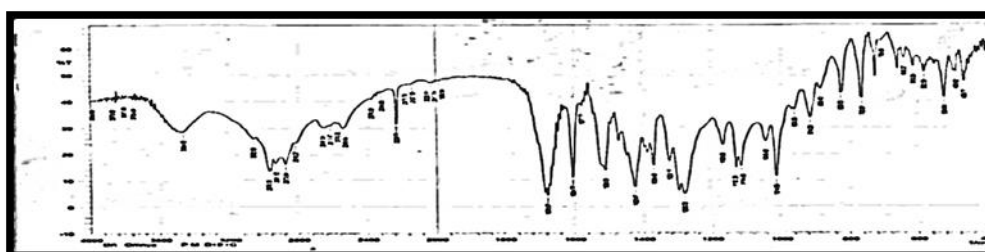
c
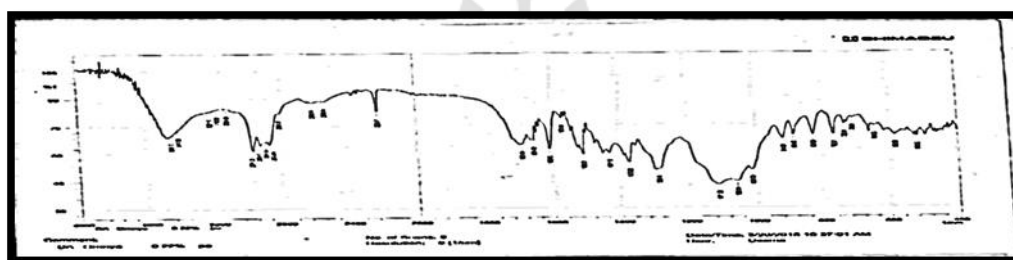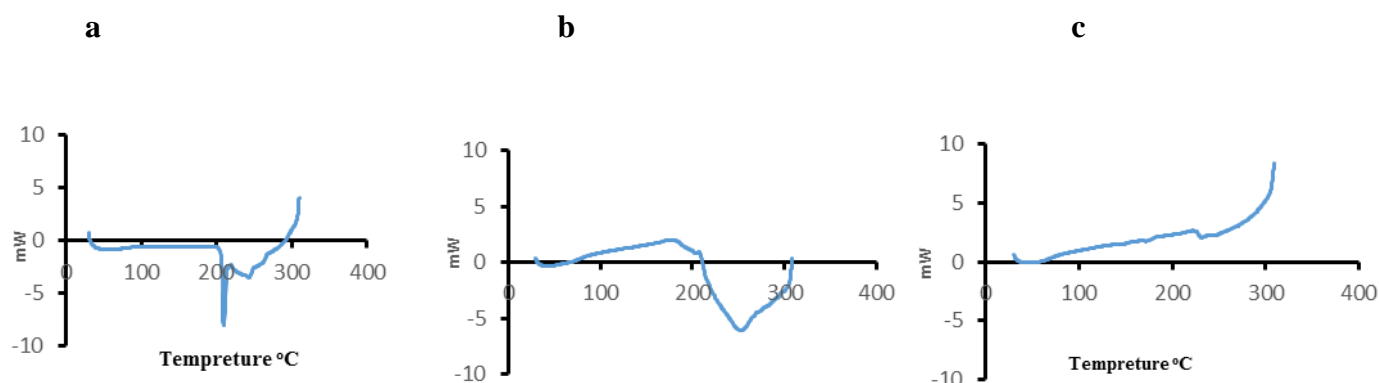

Figure No. 6: FTIR spectra of Febuxostat alone (a), Febuxostat Ethylcellulose (PM) (b) and Febuxostat loaded nanosponge (EC1) (c)

Differential Scanning Calorimetry (DSC):

Figure 7 shows the DSC thermogram of FEB alone (a) which characterized by a sharp endothermic peak at 209.3 °C corresponding to its melting point. Figure 7 (b) shows the DSC thermogram of a physical mixture of FEB and EC (PM) which is characterized by a broad endothermic peak started at 205.7 °C of FEB with corresponding heat of fusion of - 41.8 cal/g. Figure 7 (c) shows the DSC thermogram of the selected NS formula (EC$_1$) which is characterized by the disappearance of the endothermic peak of FEB indicating the successful encapsulation of drugs within the NS cavities.

Citation: Omnya M. Amin et al. Ijppr.Human, 2019; Vol. 16 (4): 309-322.

318

a   b   c

Figure No. 7: DSC thermograms of Febuxostat alone (a), Febuxostat Ethylcellulose (PM) (b) and Febuxostat loaded nanosponge (EC₁) (c)

DISCUSSION

It was observed that as the polymer ratio in the formulation increases, the percent production yield also increases (up to optimum concentration 1:6 (FEB: EC)). Further increase in the concentration of polymer (beyond the optimum level), the percent production yield was found to be decreased due to the sticky nature of the product which cannot be filtered [11]. The reason for the increase in production yield at an elevated FEB: EC ratio was abridged DCM diffusion rate from concentrated solutions to the aqueous phase, which provides additional time for the formation of droplet following improved yield. The surfactant concentration PVA in the formulation increases, the percentage yield also slightly increases for the same FEB: EC ratio [12].

It was observed that the mean amount of drug entrapped in NS was found to be lesser than the theoretical value for every drug: polymer ratio. The drug encapsulation efficiency did not attain 100%. Because some of the drugs dissolved in the aqueous phase or the used solvent. Entrapment efficiency outcomes reflected that higher FEB: EC ratios led to superior FEB loadings [11]. On the diffusion of solvents from the inner phase, almost all of the dispersed phase was transformed into solid NS and estranged particles emerged. The utmost drug loading efficiencies of these formulations could be attributed to the availability of maximum polymer amount to each drug unit in contrast to the rest of the formulations [12]. PVA concentration is indirectly proportional to the entrapment efficiency for the same FEB: EC ratio which is due to the low solubility of EC in the aqueous phase that resulted in, insufficient EC concentrations for FEB for particle encapsulation [11].

Citation: Omnya M. Amin et al. Ijppr.Human, 2019; Vol. 16 (4): 309-322.

319

All the nanosponge formulations showed particle sizes in the nano range (< 1 μm) and The mean particle size of NS was increased with increase in EC concentration which was due to a significant increase in the viscosity, thus leading to an increased droplet size and finally a higher NS size was obtained [11]. Also, the particle size was found to increase with the increase in the PVA concentration; this was due to the rise in apparent viscosity at augmented PVA concentrations [13].

It was observed that the plain Febuxostat was completely dissolved within 3 hours. The initial burst release observed for all NS formulae were ranged from 16 % to 33.72 %; can be owed to the existence of non-encapsulated drug near or on the exterior of NS. The *in-vitro* dissolution of FEB after 24 hours decline within a range of (87.55% - 44.2 %), (70.44% - 35.57 %) and (61.25% - 34.26 %) for the formulae of ($EC_1 \rightarrow EC_4$), ($EC_5 \rightarrow EC_8$) and ($EC_9 \rightarrow EC_{12}$) respectively, with respect to rise in FEB: EC ratio from 1:2 to 1:8. This is because as FEB: EC ratio has increased; for each NS, to encapsulate drug, the EC amount available was more. So, the thickening of the polymer matrix wall results in an extended diffusion path and ultimately led to lesser drug release. The highest drug release, i.e. 87.55 %, 70.44 %, and 61.25 % were found for the formulae of EC_1, EC_5, and EC_9, while the lowest drug release 44.2 %, 35.57 %, and 34.26 % was found for the formulae of EC_4, EC_8 and EC_{12} [13].

Also, it has been noted that, for all the formula containing the same (FEB: EC) ratio, the drug release went to decrease with an increasing amount of PVA. This could be attributed to the fact that the polymer matrix releases FEB after complete swelling of polymer and the time required for swelling of the polymer is directly proportional to the polymer amount in the formulation. The slight decrease in release rate with an increased amount of PVA was found to range from 87.55 % and 70.44 % to 61.25 % for formulae of EC_1, EC_5 and EC_9 (all containing 1:2 (drug: EC)) respectively [12].

These result of *in-vitro* dissolution was correlated with the results of particle size, as the particle size was increased the dissolution rate of the FEB was decreased.

The kinetic data showed that the *in vitro* dissolution of FEB from NS in phosphate buffer (PH 6.8) was followed Higuchi-Diffusion kinetic orders which express the drug dissolution from NS formulations. Based on release exponent values, it can be concluded that the formulations exhibited fickian dissolution, the same result was obtained by Mady and Ibrahim [14].

Citation: Omnya M. Amin et al. Ijppr.Human, 2019; Vol. 16 (4): 309-322.

320

Based on the dissolution study, the formulae EC_1 were exhibited burst release ($\geq$30 %) at 1st hour followed by controlling the release ($\geq$75%) at six hours, which were selected to be further characterized.

The negative sign of zeta potential indicates the stability of NS due to a higher magnitude of repulsive forces, leading to a reduction in their tendency to aggregate.

The prepared NS possesses a spherical uniform shape with a spongy structure. The presence of the fine orifices on the surface could be caused by the diffusion of the DCM from the surface of the formed nanoparticles during preparation [15].

IR spectrum of FEB alone (a) was characterized by absorption bands confirmed the structure of FEB, the same result was obtained by Han et al. [16]. FTIR spectrum of a physical mixture of FEB and EC (b) was suggested that there was no chemical interaction between drug and Ethylcellulose upon mixing them as there was not any new peak appearance or disappearance of existing peaks of the drug, discarding any chemical interaction probability among drug and EC used. The broadening and disappearance of the drug peaks in the FTIR spectrum of the selected NS formula (EC_1) (c) suggest that the drug has been successfully encapsulated in the NS core [1].

DSC thermogram of FEB alone (a) which characterized by a sharp endothermic peak corresponding to its melting point, the same result was obtained by Han et al. [16]. The results of Figure 7 (b) confirmed the results of FTIR and indicated that there was no chemical interaction between the drug and EC upon mixing them. Figure 7 (c) which is characterized by the disappearance of the endothermic peak of FEB indicating the successful encapsulation of drug within the NS cavities [1].

CONCLUSION

The nanosponges were able to complex efficiently with FEB and to control its release in physiological media. This nanosponge based formulation possesses nanosize, sponge-like structure and displays significantly better encapsulation.

ACKNOWLEDGMENTS

Citation: Omnya M. Amin et al. Ijppr.Human, 2019; Vol. 16 (4): 309-322.

321

work. I am thankful to EIPICO (Egypt) for the generous donation of EC and grateful to the Egyptian Petroleum Research Institute for the particle size & zeta potential work and Central Laboratory (Cairo University) for help in the DSC & FTIR work.

Conflict of interests:

The authors declare that they have no conflict of interests.

REFERENCES

1. Abbas N, Irfan M, Hussain A, Arshad MS, Hussain SZ, Latif S, Bukhari NI. Development and evaluation of scaffold-based nanosponge formulation for controlled drug delivery of naproxen and ibuprofen. Tropical Journal of Pharmaceutical Research. 2018;17(8):1465-74.

2. Karna S, Chaturvedi S, Agrawal V, Alim M. Formulation approaches for sustained release dosage forms: a review. Asian J Pharm Clin Res. 2015 Sep 1;8(5):46-53.

3. Ahmed RZ, Patil G, Zaheer Z. Nanosponges–a completely new nano-horizon: pharmaceutical applications and recent advances. Drug development and industrial pharmacy. 2013 Sep 1;39(9):1263-72.

4. Selvamuthukumar S, Anandam S, Krishnamoorthy K, Rajappan M. Nanosponges: A novel class of drug delivery system-review. Journal of Pharmacy & Pharmaceutical Sciences. 2012 Jan 17;15(1):103-11.

5. Szejtli J. Cyclodextrin complexed generic drugs are generally not bio-equivalent with the reference products: therefore the increase in a number of marketed drug/cyclodextrin formulations is so slow. Journal of inclusion phenomena and macrocyclic chemistry. 2005 Jun 1;52(1-2):1-1.

6. Kiliçarslan M, Baykara T. The effect of the drug/polymer ratio on the properties of the verapamil HCl loaded microspheres. Int J Pharm. 2003; 252: 99-109.

7. Asif U, Sherwani AK, Akhtar N, Shoaib MH, Hanif M, Qadir MI, Zaman M. Formulation development and optimization of febuxostat tablets by direct compression method. Advances in Polymer Technology. 2016 Jun;35(2):129-35.

8. Ahuja BK, Jena SK, Paidi SK, Bagri S, Suresh S. Formulation, optimization and in vitro–in vivo evaluation of febuxostat nanosuspension. International journal of pharmaceutics. 2015 Jan 30;478(2):540-52.

9. Dash S, Murthy PN, Nath L, Chowdhury P. Kinetic modeling on drug release from controlled drug delivery systems. Acta Pol Pharm. 2010 May 1;67(3):217-3.

10. Rao M, Bajaj A, Khole I, Munjapara G, Trotta F. In vitro and in vivo evaluation of β-cyclodextrin-based nanosponges of telmisartan. Journal of inclusion phenomena and macrocyclic chemistry. 2013 Dec 1;77(1-4):135-45.

11. Manyam N, Budideti KK, Mogili S. Formulation and in vitro evaluation of nanosponge-loaded extended-release tablets of trimethoprim. UPI J. Pharma. Med. Health Sci.. 2018;1(1):78-86.

12. Moin A, Deb TK, Osmani RA, Bhosale RR, Hani U. Fabrication, characterization, and evaluation of microsponge delivery system for facilitated fungal therapy. Journal of basic and clinical pharmacy. 2016 Mar;7(2):39.

13. Srinivas P, Sreeja K. Formulation and evaluation of voriconazole loaded nanosponges for oral and topical delivery. Int J Drug Dev Res. 2013 Jan;5(1):55-69.

14. Mady FM, Ibrahim M, Ragab S. Cyclodextrin-based nanosponge for improvement of solubility and oral bioavailability of Ellagic acid. Pakistan journal of pharmaceutical sciences. 2018 Sep 2.

15. Subhash PB, Mohite SK. Formulation design & development of Artesunate Nanosponge. Eur J Pharm Med Res 2016; 3 (5): 206. 2016;211.

16. Han X, Qi W, Dong W, Guo M, Ma P, Wang J. Preparation, optimization and in vitro–in vivo investigation for capsules of the choline salt of febuxostat. Asian journal of pharmaceutical sciences. 2016 Dec 1;11(6):715-21.

Citation: Omnya M. Amin et al. Ijppr.Human, 2019; Vol. 16 (4): 309-322.

322